A time series of SAR tomographic profiles of a snowpack

Othmar Frey
Gamma Remote Sensing, Gümligen, Switzerland / Earth Observation & Remote Sensing, ETH Zurich, Switzerland
Email: frey@gamma-rs.ch

Charles L. Werner, Rafael Caduff, Andreas Wiesmann
Gamma Remote Sensing, Gümligen, Switzerland

Abstract

Recently, the SnowScat hardware—a tower-mounted fully-polarimetric scatterometer at X-/Ku-band—has been enhanced to also provide a tomographic profiling mode which allows to obtain high-resolution 2-D vertical profiles that may provide further insights into the electromagnetic interaction within layered snowpacks. In winter 2014/2015, a first test campaign was carried out yielding a successful proof of concept of the hardware, tomographic measurement, and basic processing concept. As a follow-up, in Nov/Dec 2015, the SnowScat device was installed at a test site on 1700m altitude close to the Grimsel pass in Switzerland. Since then it has been acquiring a time series of tomographic profiles of a snow pack. In this paper, we present and discuss first results of this new time series.

1 Introduction

The SnowScat system, a tower-mounted fully-polarimetric scatterometer at X-band up to Ku-band [1, 2], was recently enhanced with an additional high-resolution tomographic profiling mode with the aim to facilitate non-destructive high-resolution measurements of the stratification of snow and to investigate the complex electromagnetic interaction within snowpacks. A first field campaign carried out with the SnowScat system operated in tomographic profiling mode was carried out during winter 2014/2015. Within this campaign the proof of concept was demonstrated and first tomographic profiles were obtained and compared to in-situ measurements of the stratification of the snowpack. We have presented first results of that campaign in [3, 4]. Similar ground-based tomographic experiments with different hardware and configuration were also reported in [5, 6, 7, 8]. In the past winter season 2015/2016, a more comprehensive field campaign has been taking place during which an extended time series of tomographic profiles and accompanying in-situ measurements of a snowpack has been acquired with typically two to three tomographic profiles acquired with the SnowScat device per day. First results obtained from processing and analysing excerpts this new time series of tomographic profiles of a snowpack are presented in this paper.

Table 1: List of variables

x_r	horiz. pos. of antenna phase center
z_r	height of antenna phase center (APC) above ground level
x_p	horizontal position of target
z_p	height of target pos. above ground
z_s	depth of snow layer
$d_a = z_r - z_s$	vert. distance between APC and top of snow layer
$d_s = z_s - z_p$	vertical distance between top of snow layer and target position
$d_{a/s} = z_s - z_p$	horiz. distance between APC and target position
$r_a = \sqrt{{d_a}^2 + {d_{a/s}}^2}$	slant range between APC and point of entry at air-snow interface
$d_p = x_p - x_r$	horizontal distance between APC and target position
$r_s = \sqrt{(d_p - d_{a/s})^2 + {d_s}^2}$	slant range between point of entry at air-snow interface and target
n_a	refractive index of air
n_s	refractive index of homog. snow layer (assumed as initial condition)
c_a	propagation velocity in air
c_s	propagation velocity in homog. snow layer (assumption)
$x_{a/s} =?$	horiz. pos. of air-snow interface (to be solved for each APC-target pos. pair)
θ_a	angle of incidence in air at the air/snow interface
θ_s	angle of incidence in the snow at the air/snow interface

2 Methods

We start by introducing the methodology for tomographic processing, which has been applied so far and which is the basis for further refinements of the processing that may be required in the presence of larger snow depths and multiple snow layers. To improve the readability of this section we provide a list of variables (see Table 1).

2.1 Tomographic processing

The vertical snow profiles are obtained by a time-domain back-projection (TDBP) approach [9], i.e., through aperture synthesis along the elevation direction.

The calculation of the point of entry is based on the following trigonometric relationships:

ISBN 978-3-8007-4228-8 / ISSN 2197-4403

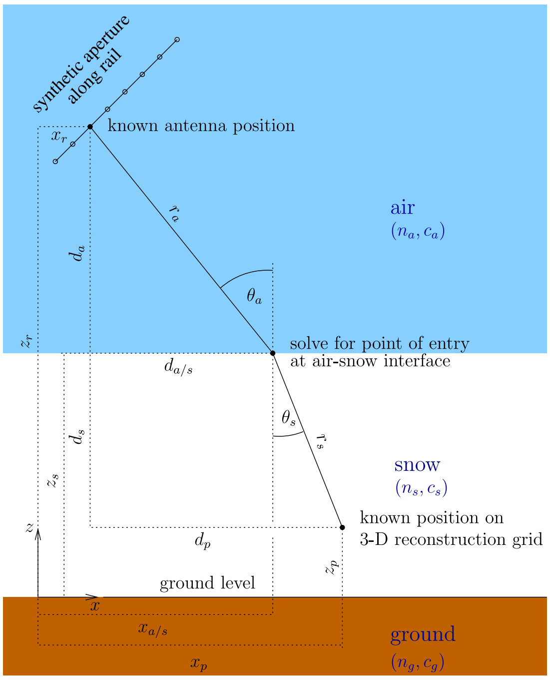

Figure 1: Sketch of simplified acquisition scenario for tomographic profiling of a snowpack with the SnowScat device.

$$\sin\theta_a = \frac{d_{a/s}}{\sqrt{d_{a/s}^2 + d_a^2}} \quad (1)$$

$$\sin\theta_s = \frac{d_p - d_{a/s}}{\sqrt{(d_p - d_{a/s})^2 + d_s^2}} \quad (2)$$

and Snell's law :

$$\frac{\sin\theta_a}{\sin\theta_s} = \frac{n_s}{n_a} \quad (3)$$

The TDBP processing employed is essentially a ray-tracing approach that takes into account a simplified refraction model assuming one homogeneous snow layer with refraction occurring at the air/snow interface. The calculation of the point of entry at the air/snow interface is based on the trigonometric relationships as depicted in Fig. 1. A virtual range distance R_v that corresponds to the actual time delay in the radar echo can be expressed follows (using the terms given in Fig. 1 and Table 1):

$$R_v = n_a\sqrt{d_{a/s}^2 + d_a^2} + n_s\sqrt{(d_p - d_{a/s})^2 + d_s^2}. \quad (4)$$

In a more general form, the TDBP aperture synthesis along the elevation direction can then be written as:

$$v(\vec{r}_i) = \sum_{k=1}^{M} g_k[R_v(\vec{r}_i, \vec{r}_k, n_s)] \cdot \exp[i\, 4\pi/\lambda R_v(\vec{r}_i, \vec{r}_k, n_s)] \,, \quad (5)$$

where $\vec{r}_i$ is the 3-D position vector of the target location for which the tomographic inversion is performed, $\vec{r}_k$ is the 3-D position vector of the antenna phase centre at position k within the synthetic aperture, $g_k(\ldots)$ is the range-compressed signal at antenna position k, λ is the wavelength of the carrier signal, $R_v(\vec{r}_i, \vec{r}_k, n_s)$ is the (virtual) range distance between antenna position k and the location $\vec{r}_i$ using the simple refraction model, and $v(\vec{r}_i)$ is the focused signal at location $\vec{r}_i$.

Table 2: System specifications of the SnowScat device in tomographic profiling mode during the SnowLab experiment at the testsite Gerstenegg, winter 2015/2016

Frequency	SFCW from 9.2 to 17.8GHz
Incidence angle	-40^o to 110^o
Azimuth angle	-180^o to 180^o
Sampling spacing	0.04 m
Number of samples	50
Synth. aperture length	1.94 m
3dB res. (stripmap m.)	0.15 m
Power	230V, max $\sim$ 60W
Weight	$\sim$ 40 kg
Temperature range	-40^{o}C to 40^{o}C
Antennas	Dual pol, $<$ 10^o (3dB)
Antenna cross-pol	$<$ -25dB
Polarization	HH, HV, VV, VH
Dynamic range	Receiver dynamic range $>$ 80dB with the 16bit ADC
Signal bias	$<$ 0.5dB
Gain characterization	Internal calibration, calibration sphere (Ø = 255mm)
RFI	Frequency blacklist

2.2 Experimental setup for tomographic profiling

Fig. 2 (a) and (b) show the hardware setup in tomographic profiling mode as implemented at the test site Gerstenegg on 1700m altitude close to the Grimsel pass in the Swiss Alps, in January 2015. In Table 2 the system parameters of the enhanced SnowScat device are provided. The SnowScat device is attached to a rail on a triangular truss, which again is mounted onto a scaffold (see Fig. 2(a)). In tomographic profiling mode, the SnowScat is subsequently moved along this rail within a total synthetic aperture length of about 2 m. The tomographic test target (Fig. 2(b)) is used as a reference target in snow-free as well as under snow condition.

Fig. 2(c) shows an overview of the new test site Gerstenegg (2015/2016 campaign) with the tower (scaffolding), the local meteo station, the area for the SnowScat tomographic profiling of the snow volume, and the adjacent area for accompanying in-situ snow profile measurements. The test site also hosts a weather station to provide in-situ measurements of temperature, wind speed, humidity, solar radiation and snow height.

A time-series of tomographic measurements over almost an entire snow season (January until end of March) has been built up as part of the SnowLab experiment: typically, two to three tomographic measurement cycles were performed with the SnowScat device, per day.

3 Results

In Fig. 3, tomographic profiles obtained by TDBP-focusing of 50 SnowScat radar echoes (HH-channel) are shown: Measurements of the tomographic test target with its 8 aluminium spheres are given in different snow pack conditions at three different dates Feb. 23, Mar. 11,

ISBN 978-3-8007-4228-8 / ISSN 2197-4403

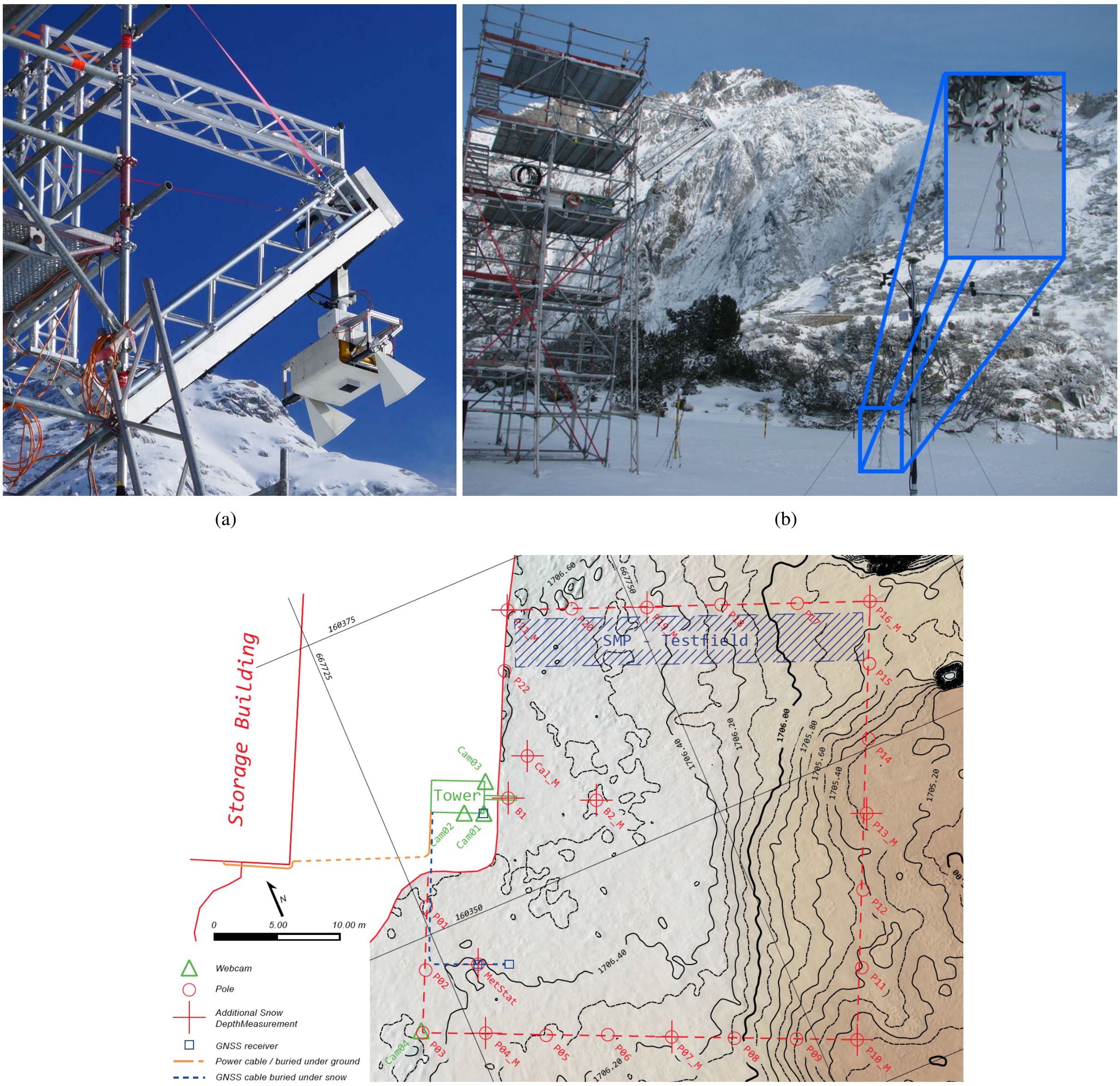

(a) (b)

(c)

Figure 2: (a) and (b): SnowLab experimental setup at the testsite Gerstenegg, Switzerland, in January, 2016. For tomographic profiling measurements, the SnowScat device is moved along the rail taking 50 measurements at intervals of 4cm). A tomographic target is used (see close-up view) with its vertical array of eight spheres. The synthetic aperture in elevation direction is formed by taking subsequent measurements at different positions along the rail. The upper edge of the truss to which the rail is attached is situated approximately 10m above ground. The pointing direction of the SnowScat antennas is adjustable in elevation and azimuth. (a) Close-up of the SnowScat device during tomographic data acquisition. (b) Overview of the entire measurement setup with a close-up of the tomographic test target. (c) Overview of the new test site Gerstenegg (2015/2016 campaign) with the tower (scaffolding), the local meteo station, the area for the SnowScat tomographic profiling of the snow volume, and the adjacent area for accompanying in-situ snow profile measurements.

and Mar. 18, 2016. All data sets were acquired at the SnowLab test site Gerstenegg (1700 m.s.l.), Switzerland.

In the left column of Fig. 3 focused tomographic profiles without considering refraction are shown. In the mid-left column, the focused tomographic profiles of the same data sets are depicted, however with a first order correction of the refraction applied during focusing. Fig. 3 also contains (1) the respective close-ups of the tomographic test target, which give a good estimate of the actual in-situ snow height, and (2) snow profiles taken nearby on the test site at the same day as the SnowScat measurements.

4 Discussion & Outlook

The first acquisition (2016-02-23) shows a situation with virtually no penetration into the snow pack. Underlying structures can therefore not be detected. The acquisitions from 2016-03-11 and 2016-03-18 show situations

ISBN 978-3-8007-4228-8 / ISSN 2197-4403

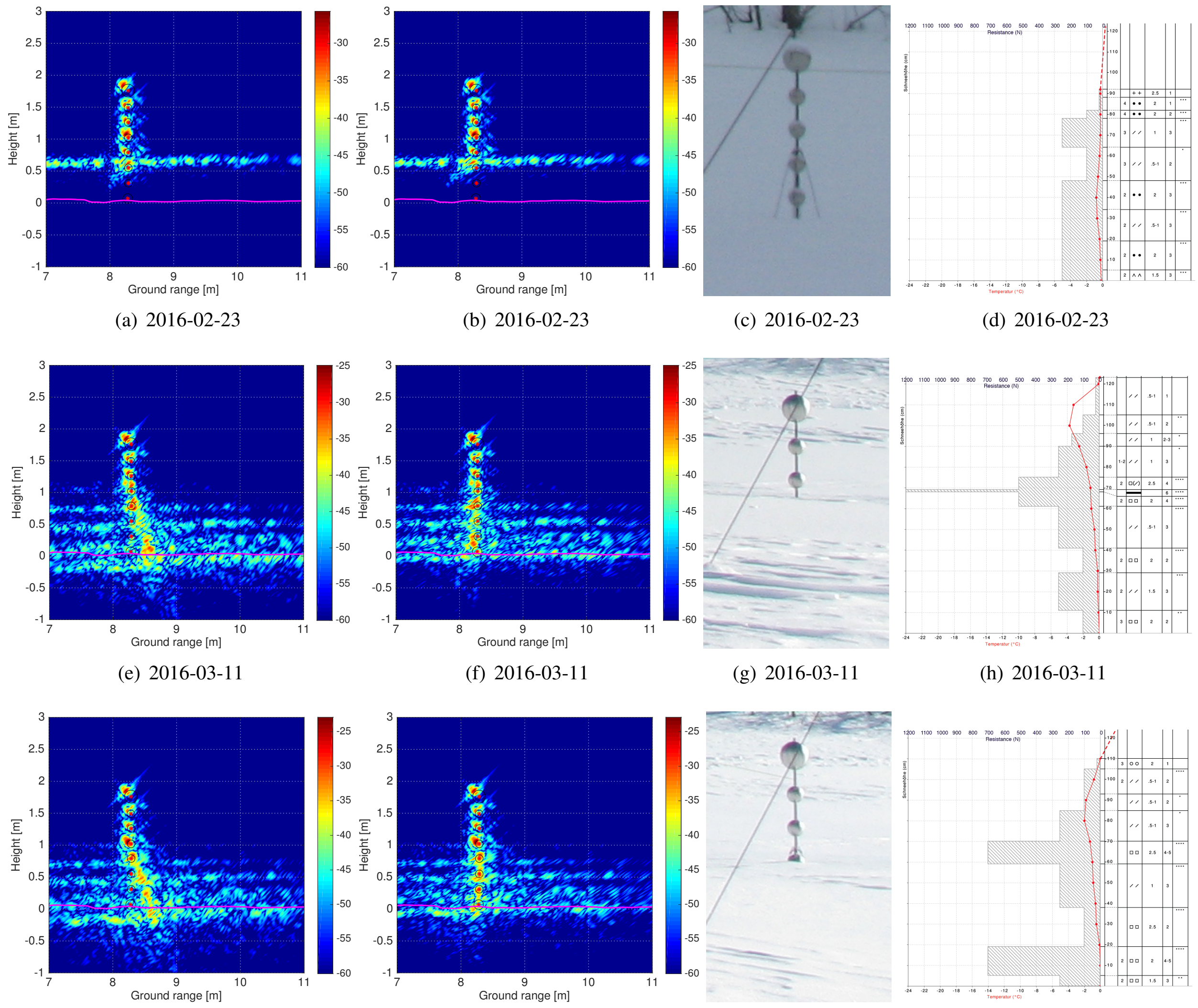

(a) 2016-02-23 (b) 2016-02-23 (c) 2016-02-23 (d) 2016-02-23

(e) 2016-03-11 (f) 2016-03-11 (g) 2016-03-11 (h) 2016-03-11

(i) 2016-03-18 (j) 2016-03-18 (k) 2016-03-18 (l) 2016-03-18

Figure 3: Left column (a), (e), (i): focused tomographic profiles with nominal focusing (no refraction considered). Each profile is obtained from 50 SnowScat measurements taken along the rail. The data sets were acquired at the test site Gerstenegg (1700 m.s.l.), Switzerland, three different dates (2016-02-23, 2016-03-11, and 2016-03-18).
Mid-left column (b), (f), (j): the same focused tomographic profiles when applying a first order correction of the refraction during focusing.
Mid-right column (c), (g), (k): close-up of the tomographic test target indicating the actual in-situ snow height.
Right column (d), (h), (l): snow profiles taken nearby on the test site at the same day as the SnowScat measurements.

with snow depths of about 1m to 1.2m and a complete penetration into the snow volume down to the ground. Several horizontal layers with pronounced backscattering can be observed. It is also interesting to note that the lower layers and the ground that are visible in these tomographic profiles were already visible in tomographic profiles taken previously in January and early February; they were then temporarily hidden, as expected, when melting occurred at the snow surface (the situation shown on 2016-02-23). A first comparison of the tomographic profiles and the in-situ profiles taken at this test site indicate that, depending on the snow condition and the spatial heterogeneity of the snow cover, a direct validation of the tomographic profiles with in-situ snow profiles may be difficult (the spatial heterogeneity of the snow depth at the test site was also confirmed by additional close-range photogrammetry-based DEM differencing).
Since, as of today, the SnowScat device has been still acquiring data the analysis of the complete time-series is still ongoing.

Acknowledgment

The SnowScat hardware extension was built and tested in the frame of ESA/ ESTEC Contract No. 20716/06/NL/EL CCN3, “Enhancement of SnowScat for tomographic and vertical profiling observation capabilities”. A. Henzen at KWO hydroelectric power company, Innertkirchen, Switzerland is gratefully acknowledged for hosting the SnowLab test site Gerstenegg and for supporting the in-situ measurements. M. Schneebeli and M. Jaggi at SLF, Davos, Switzerland are gratefully acknowledged for the in-situ snow profile measurements.

References

[1] C. L. Werner, A. Wiesmann, T. Strozzi, M. Schneebeli, and C. Matzler, "The SnowScat ground-based polarimetric scatterometer: Calibration and initial measurements from Davos Switzerland," in *Proc. IEEE Int. Geosci. Remote Sens. Symp.*, July 2010, pp. 2363–2366.

[2] A. Wiesmann, C. L. Werner, C. Matzler, M. Schneebeli, T. Strozzi, and U. Wegmuller, "Mobile X- to Ku-band scatterometer in support of the CoRe-H2O mission," in *Proc. IEEE Int. Geosci. Remote Sens. Symp.*, vol. 5, July 2008, pp. 244–247.

[3] O. Frey, C. L. Werner, M. Schneebeli, A. Macfarlane, and A. Wiesmann, "Enhancement of SnowScat for tomographic observation capabilities," in *Proc. FRINGE 2015*, ser. ESA SP-731, Mar. 2015.

[4] O. Frey, C. L. Werner, and A. Wiesmann, "Tomographic profiling of the structure of a snow pack at X-/Ku-band using SnowScat in SAR mode," in *Proc. EuRAD 2015 - 12th European Radar Conference*, Sept. 2015, pp. 21–24.

[5] S. Tebaldini and L. Ferro-Famil, "High resolution three-dimensional imaging of a snowpack from ground-based SAR data acquired at X and Ku band," in *Proc. IEEE Int. Geosci. Remote Sens. Symp.*, July 2013, pp. 77–80.

[6] L. Ferro-Famil, S. Tebaldini, M. Davy, and F. Boute, "3D SAR imaging of the snowpack at X- and Ku-band: results from the AlpSAR campaign," in *Proc. of EUSAR 2014 - 10th European Conference on Synthetic Aperture Radar*, June 2014, pp. 1–4.

[7] K. Morrison and J. Bennett, "Tomographic profiling - a technique for multi-incidence-angle retrieval of the vertical SAR backscattering profiles of biogeophysical targets," *IEEE Trans. Geosci. Remote Sens.*, vol. 52, no. 2, pp. 1350–1355, Feb. 2014.

[8] B. Rekioua, M. Davy, and L. Ferro-Famil, "Snowpack characterization using sar tomography - experimental results of the alpsar campaign," in *Radar Conference (EuRAD), 2015 European*, Sept 2015, pp. 33–36.

[9] O. Frey and E. Meier, "3-D time-domain SAR imaging of a forest using airborne multibaseline data at L- and P-bands," *IEEE Trans. Geosci. Remote Sens.*, vol. 49, no. 10, pp. 3660–3664, Oct. 2011.

